© 2021. Published by The Company of Biologists Ltd | Journal of Cell Science (2021) 134, jcs254995. doi:10.1242/jcs.254995

RESEARCH ARTICLE

Identification of additional outer segment targeting signals in zebrafish rod opsin

Xiaoming Fang[1], Andrew A. Peden[2], Fredericus J. M. van Eeden[1,*] and Jarema J. Malicki[1,‡]

ABSTRACT

In vertebrate photoreceptors, opsins are highly concentrated in a morphologically distinct ciliary compartment known as the outer segment (OS). Opsin is synthesized in the cell body and transported to the OS at a remarkable rate of 100 to 1000 molecules per second. Opsin transport defects contribute to photoreceptor loss and blindness in human ciliopathies. Previous studies revealed that the rhodopsin C-terminal tail, of 44 amino acids, is sufficient to mediate OS targeting in *Xenopus* photoreceptors. Here, we show that, although the *Xenopus* C-terminus retains this function in zebrafish, the homologous zebrafish sequence is not sufficient to target opsin to the OS. This functional difference is largely caused by a change of a single amino acid present in *Xenopus* but not in other vertebrates examined. Furthermore, we find that sequences in the third intracellular cytoplasmic loop (IC3) and adjacent regions of transmembrane helices 6 and 7 are also necessary for opsin transport in zebrafish. Combined with the cytoplasmic tail, these sequences are sufficient to target opsin to the ciliary compartment.

KEY WORDS: Opsin, Cilia, G-protein-coupled receptors, Photoreceptor, Vision

INTRODUCTION

Vertebrate photoreceptors detect light via a specialized cilium that contains hundreds of parallel membrane folds harboring the photosensitive pigment opsin and other components of the phototransduction cascade. It is estimated that 10^8-10^9 opsin molecules are tightly packed in the ciliary membranes of a single photoreceptor cell (Pugh and Lamb, 2000). Opsin is the main protein component of photoreceptor cilia, and in addition to detecting light its presence is also essential for cilia morphogenesis (Lem et al., 1999; Pugh and Lamb, 2000). Photosensitive membranes of photoreceptors are continuously turned over: they are shed from the distal end of the cilium while new membrane folds are added to the cilium base (Young, 1967; Young and Droz, 1968). In the mouse retina, this process replaces ∼10% of the photoreceptor ciliary membranes every day (LaVail, 1973). Consequently, 10% of all protein content of the cilium, including opsins and other phototransduction cascade components, are transported into the cilium every day.

The complex architecture of photosensitive membranes results in an unusually large volume of photoreceptor cilia (reviewed by Kennedy and Malicki, 2009). The bulk of the cilium, referred to as the outer segment (OS), connects to the cell body via a narrow stalk, termed the connecting cilium, characterized by the typical architecture and dimensions of the ciliary transition zone (Tokuyasu and Yamada, 1959; Nilsson, 1964; Besharse et al., 1985; Röhlich, 1975). All proteins destined for the OS, including opsins, are transported through the connecting cilium (reviewed by Kennedy and Malicki, 2009, Malicki and Besharse, 2012). Given the unusually large size of the OS and its high protein content, transport into the photoreceptor cilium requires a particularly efficient mechanism (Malicki and Besharse, 2012).

Many attempts have been made to gain insight into the mechanism of rod opsin transport. A key finding in this area is that the cytoplasmic tail of 44 amino acids of rod opsin (hereafter CT44) is sufficient to mediate transport into the *Xenopus* OS (Tam et al., 2000). Human mutations in the homologous sequence lead to rapid vision loss (Sung et al., 1991; Bessant et al., 1999; Berson et al., 2002, reviewed by Athanasiou et al., 2018; Sung et al., 1994), which further speaks to its importance. To direct transport, rod opsin C-terminal sequences must interact with protein components of cytoplasmic and/or ciliary transport machinery. Although some proteins that bind CT44 have been identified using biochemical approaches (Deretic et al., 2005; Mazelova et al., 2009; Wang et al., 2012; Tai et al., 1999; Chuang et al., 2007; Keady et al., 2011), the understanding of this process is far from complete. How such a functionally diverse group of proteins contributes to opsin transport requires further investigation. It is also noteworthy that based on previous analyses, opsin appeared to differ from other ciliary G-protein-coupled receptors (GPCRs), which contain a cilia targeting sequence (CTS) in the third intracellular loop and do not display obvious homologies to opsin C-terminal targeting motifs (Berbari et al., 2008).

Here, we further characterize rod opsin OS targeting. Surprisingly, we find that although *Xenopus* CT44 is sufficient to target an exogenous protein, such as GFP, to the ciliary compartment of zebrafish photoreceptors, the homologous zebrafish sequence is unable to do so. A single amino acid in the opsin helix 8 is predominantly responsible for this difference. This suggests that additional sequences are necessary to target rod opsins to the OS. Indeed, the analysis of Opsin/Sstr5 hybrid constructs reveals that a targeting sequence exists in the third intracellular cytoplasmic loop (IC3) of rod opsin. Deletion of this motif causes opsin transport deficiency. Rod opsin ciliary targeting also requires parts of two transmembrane helices that flank the third cytoplasmic loop. These studies have uncovered novel motifs necessary to target rod opsin to the ciliary compartment of the photoreceptor in zebrafish and may allow for the identification of machinery involved in its transport in the future.

RESULTS

Construction of transgenic tools to monitor opsin transport

To monitor the dynamics of opsin transport *in vivo*, we generated stable zebrafish transgenic lines that express an EGFP-opsin fusion specifically in rod photoreceptors from an inducible promoter. This

[1]Bateson Centre and Department of Biomedical Science, University of Sheffield, Firth Court, Western Bank, Sheffield, S10 2TN, UK. [2]Department of Biomedical Science, University of Sheffield, Firth Court, Western Bank, Sheffield, S10 2TN, UK. ‡Deceased

*Author for correspondence (f.j.vaneeden@sheffield.ac.uk)

F.J.M.v.E., 0000-0003-3483-8269; J.J.M., 0000-0002-5947-8805

Handling Editor: David Stephens
Received 30 September 2020; Accepted 1 February 2021

Journal of Cell Science (2021) 134, jcs254995. doi:10.1242/jcs.254995

system provides both spatial and temporal control of opsin expression. It consists of two transgenic lines: (1) a line that specifically expresses Cre recombinase in photoreceptors from the rhodopsin promoter, and (2) a temperature-inducible line that conditionally expresses EGFP-S-opsinCT44 (EGFP fused with S-peptide and *Xenopus* CT44) from a heat shock promoter (Fig. 1A-C). A lox-mCherry-STOP-lox cassette is inserted upstream of EGFP-S-opsinCT44 in this line. When these two lines are crossed, Cre induces recombination specifically in rod photoreceptors, placing EGFP-S-opsinCT44 under the control of a heat shock promoter (Fig. 1A). When heat shock was applied, embryos expressed EGFP-S-opsinCT44 specifically in rods and mCherry in all other cells (Fig. 1D,E). The EGFP-S-opsinCT44 fusion protein was efficiently transported to photoreceptor outer segments in these animals (Fig. 1E,I). In a control line, which contains 44 random amino acids in place of the 44 amino acids from the rhodopsin C-terminus, the EGFP signal is no longer enriched in the OS and instead is present throughout the entire photoreceptor cytoplasm (Fig. 1F).

Zebrafish and *Xenopus* CT44 differ in their ability to opsin transport

In *Xenopus*, CT44 is sufficient to mediate rhodopsin OS targeting (Tam et al., 2000). To evaluate the function of the zebrafish opsin C-terminal region in OS-directed transport, we fused the 44 C-terminal amino acids of zebrafish rod opsin to EGFP and expressed it from a heat shock promoter using stable transgenic lines, as previously described for *Xenopus* CT44 (Fig. 1). We compared EGFP transport efficiency in these lines to that in animals containing *Xenopus* CT44 transgene by assessing EGFP intensity in the cell body. We measured EGFP fluorescence in the cell body rather than the OS, because the signal in the OS becomes saturated quickly, decreasing sensitivity of our measurements. Surprisingly, we found that in contrast to the *Xenopus* C-terminus (XCT44), the equivalent region of zebrafish opsin (ZCT44) is very inefficient at targeting opsin to the zebrafish photoreceptor OS (Fig. 1G-I). Similar results were also obtained using a transient expression assay, in which we also used a heat shock promoter to generate a pulse of GFP-CT44 expression and monitor the rate at

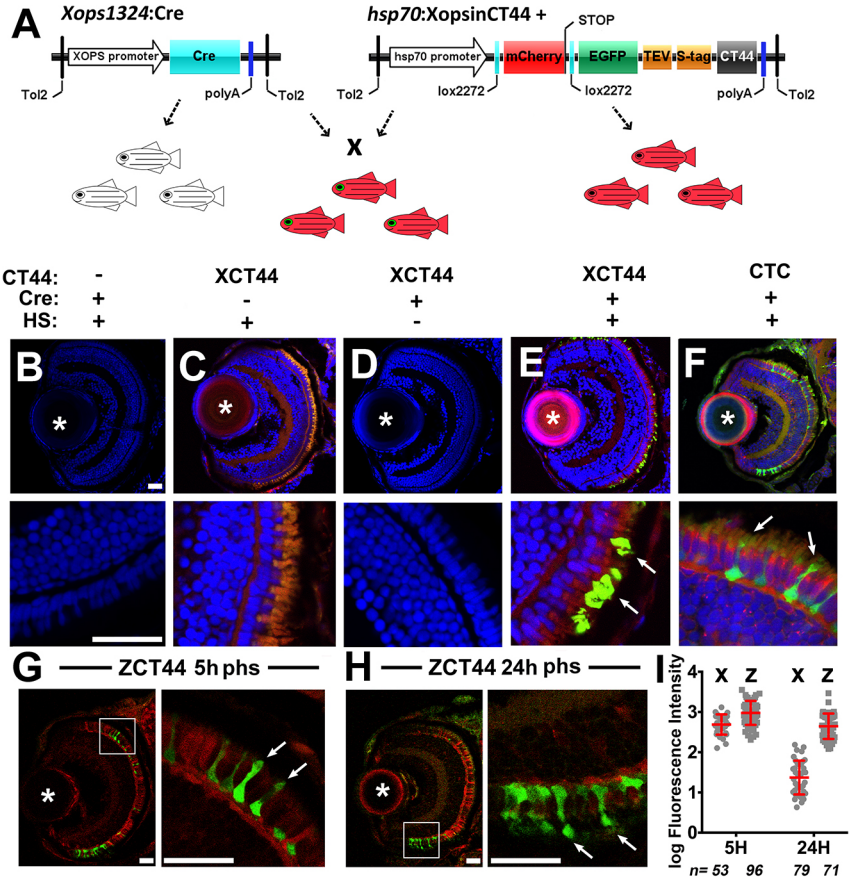

Fig. 1. A transgenic zebrafish system monitors opsin transport in rod photoreceptors. (A) Schematic of transgenes used to obtain spatial and temporal control of expression for EGFP-S-opsinCT44 fusion proteins. (B-H) Confocal images of cryosections through the retinae of transgenic zebrafish larvae at 5 dpf. In B-F, the lower panels show higher magnification images. Transgene genotypes and heat shock treatment are indicated above. CTC, control random 44 amino acid peptide. (B) No fluorescent signal was observed in the Cre line even when heat shock was applied. (C) mCherry but not GFP expression was present when heat shock was applied to the hsp70:(mCherry)EGFP-S-opsinXCT44 transgenic line. (D) No fluorescent signal was observed in the double transgenic line when heat shock was not applied. (E) EGFP was expressed in photoreceptors but not in other retinal cells when heat shock was applied to the double transgenic line containing Tg(XOPS-1324:Cre) and Tg(hsp70: lox2272-mCherry-lox2272-EGFP-2xTEV-S-tag-XCT44) transgenes. EGFP signal localized to OSs in this line (arrows in lower panels). (F) In contrast, EGFP signal remained in the cell body in a double transgenic line that contained a control EGFP construct in which CT44 cilia targeting signal was replaced with a random peptide. (G,H) High level of EGFP-S-opsinZCT44 persisted in the photoreceptor cell body at 5 h (G) and 12 h (H) after heat shock (phs, post heat shock). Panels to the right show enlargements of photoreceptors from images presented to the left. (I) GFP signal intensity in the cell body at 5 h and 24 h post heat shock for *Xenopus* (X) and zebrafish (Z) GFP-CT44 fusions. Log-transformed data from two independent experiments are shown. Each dot represents a measurement from a single photoreceptor cell. GFP is efficiently transported from the cell body to the OS when using the *Xenopus* but not the zebrafish CT44 (P<0.001, ANOVA). Error bars represent the s.d. In B-F, sections are counterstained with DAPI (blue). The scale bar in the upper panel of B also applies to the upper panels of C-F. The scale bar in the lower panel of B also applies to the lower panels of C-F. Scale bars: 25 µm. Asterisks indicate the lens.

Journal of Cell Science

Journal of Cell Science (2021) 134, jcs254995. doi:10.1242/jcs.254995

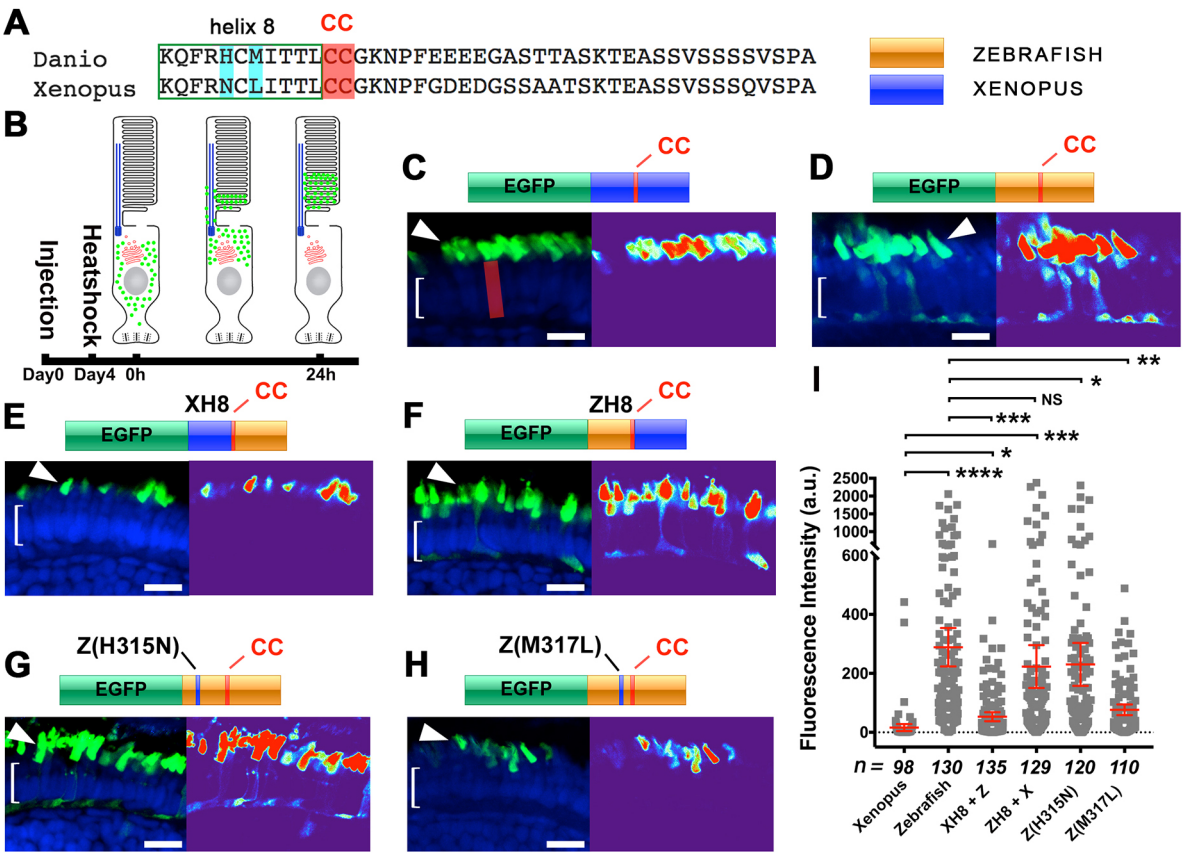

Fig. 2. Comparison of OS-targeting efficiency of *Xenopus* and zebrafish opsin C-terminal tails. (A) Alignment of rod opsin 44 C terminal amino acids from zebrafish and *Xenopus*. Palmitoylated cysteines are highlighted in red. (B) A schematic demonstrating the process of the transient assay. (C-H) Confocal images of cryosections through the photoreceptor cell layer of wild-type zebrafish retinae that transiently express the following variants of the EGFP-CT44 construct at 5 dpf: (C) XCT44, (D) ZCT44, (E) ZCT H8+X, (F) XCT H8+Z, (G) Z-H315N and (H) Z-M317L. Confocal image (left) and a heat map (right) of GFP signal intensity are juxtaposed. Brackets indicate the photoreceptor cell layer, and arrowheads point to OSs. (I) Quantification of fluorescence intensity in photoreceptor cell bodies. The red rectangle in C approximately shows the soma of a single photoreceptor cell. Each dot represents a measurement from a single photoreceptor cell. Data are mean±95% c.i. from three independent experiments. Sample sizes are provided in italics below the horizontal axis. In schematic drawings above panels C-H, zebrafish and *Xenopus* sequences are color-coded in orange and blue, respectively. Red bars indicate conserved cysteine residues in the rod opsin C terminus. Data are log transformed for statistical analysis as described in Materials and Methods. *<0.05; **<0.01; ***<0.001; ****<0.0001; ns, not significant (ANOVA). a.u., arbitrary units. Scale bars: 10 µm.

which opsin-GFP is cleared from the photoreceptor cell body (Zhao and Malicki, 2011) (Fig. 2B-D). These results indicate that, unexpectedly, opsin targeting mechanisms differ significantly among vertebrate species.

The 44 C-terminal amino acids of the rod opsin sequence contain an α-helical region, referred to as the helix 8, flanked on the C-terminal side by a pair of cysteines (Fig. 2A) (Palczewski et al., 2000). Several studies suggested that helix 8 mediates opsin dimerization, which, in turn, may play a role in opsin transport (Knepp et al., 2012; Zhang et al., 2016). We therefore hypothesized that helix 8 is responsible for differences in opsin transport efficiency between the zebrafish (ZCT44) and *Xenopus* (XCT44) C-terminal regions. To test this, we replaced helix 8 in the zebrafish C-terminal cytoplasmic tail with the *Xenopus* sequence (Fig. 2E) and, vice versa, we substituted helix 8 of the *Xenopus* C-terminal tail with the zebrafish sequence (Fig. 2F). The *Xenopus* helix 8 very significantly improved the transport efficiency of ZCT44 (Fig. 2E,I; $P<0.001$). Consistent with that, replacing *Xenopus* CT44 helix 8 with the zebrafish sequence strongly decreased targeting efficiency (Fig. 2F,I; $P<0.001$). *Xenopus* sequences outside helix 8 affect opsin targeting to a lesser degree: replacing the C-terminal sequence of zebrafish ZCT44 with the *Xenopus* sequence did not result in a significant difference (compare Fig. 2. D-F and I). Replacing the same fragment of *Xenopus* CT44 with the zebrafish sequence did, however, somewhat decrease targeting efficiency (Fig. 2E,I; $P<0.05$). These results demonstrate that helix 8 is of paramount importance for the OS targeting of rod opsin.

Rod opsin helix 8 is very well conserved across vertebrate phyla (Fig. S1). Zebrafish and *Xenopus* helix 8 sequences differ only at two positions: 315 and 317 (Fig. 2A). To narrow down which amino acid contributes to opsin targeting efficiency the most, we substituted single amino acids in zebrafish helix 8 with *Xenopus* ones. We found that although H315N substitution altered transport relatively weakly ($P<0.05$) (Fig. 2G,I), the substitution of methionine 317 with leucine (M317L) significantly improved transport efficiency (Fig. 2H,I; $P<0.01$). Sequence comparison of rod opsins from over 20 vertebrate species reveals that position 317 is almost invariably occupied by methionine (Fig. S1). The sole exception among these species is *Xenopus*. To test whether the exceptional targeting ability of XCT44 is due to the presence of the leucine, we introduced the sequence of human rod opsin C-terminus (HCT38) to the transient assay (Fig. S2A-D). In line with the zebrafish CT44, the targeting deficiency of human CT38, compared to *Xenopus* CT44, was significantly improved by its M317L substitution (Fig. S2B-D,G). We were curious how Leu317 would behave in non-opsin GPCRs. To address this question, we replaced the entire helix 8 in XCT44 with

Journal of Cell Science (2021) 134, jcs254995. doi:10.1242/jcs.254995

the C-terminal sequence of porcine α adrenergic receptor (Standfuss et al., 2011), which is a GPCR that shares structural similarities with rod opsin. This chimera, which is supposed to localize to the *Xenopus* OS (Tam et al., 2000), was found mainly in the cell body and the synapse of zebrafish photoreceptors. Strikingly, the substitution of phenylalanine with leucine also enhanced the OS targeting to a significant level (Fig. S2E-G). Given the importance of this amino acid in opsin targeting (Fig. 2I), our findings show that *Xenopus* CT44 transport into the outer segment is mediated by different molecular interactions, compared to that of zebrafish CT44, and highly likely compared to most other vertebrate rod opsins. Importantly, these findings reveal that, in addition to the C-terminus, other opsin sequences are necessary to target opsin to the outer segment.

Additional opsin ciliary targeting motifs

To search for additional OS-targeting signals in the opsin sequence, we constructed a series of hybrid GPCRs combining sequences from zebrafish rod opsin and another GPCR, Sstr5. We chose Sstr5 because unlike its close relative, SSTR3, it is not targeted to cilia (Berbari et al., 2008). All constructs were transiently expressed from a heat shock promoter as above. Compared to opsin, Sstr5 is transported to the photoreceptor ciliary outer segment very inefficiently (Fig. 3A,B; compare constructs 1 and 2). Substitution of Sstr5 C-terminal cytoplasmic tail with zebrafish CT44 did not result in a significant improvement of transport efficiency (construct 3, Fig. 3A,B). The deficiency was preserved when we replaced the Sstr5 sequence with a non-OS-targeted photopigment sequence (Melanopsin-A, Opn4a; Fig. S3A,B; Matos-Cruz et al., 2011; Davies et al., 2011), which is able to reach the plasma membrane with no issues (Fig. S3C,D). Analysis of four additional hybrid constructs revealed that transport efficiency correlates with the presence of IC3, which is the equivalent region in which several other ciliary targeting motifs of GPCRs are also found (Berbari et al., 2008; Loktev and Jackson, 2013; Nagata et al., 2013) (Fig. 3A,B; constructs 4-7). Consistently, replacement of this loop with the Sstr5 sequence resulted in a dramatic loss of transport efficiency (Fig. 3A,B; compare constructs 2 to 8). These studies show that IC3 is required for opsin targeting to the OS.

The assay that we used to monitor opsin transport efficiency into the ciliary compartment measures the rate of GFP signal loss in the photoreceptor cell body. In addition to OS-directed transport, loss of

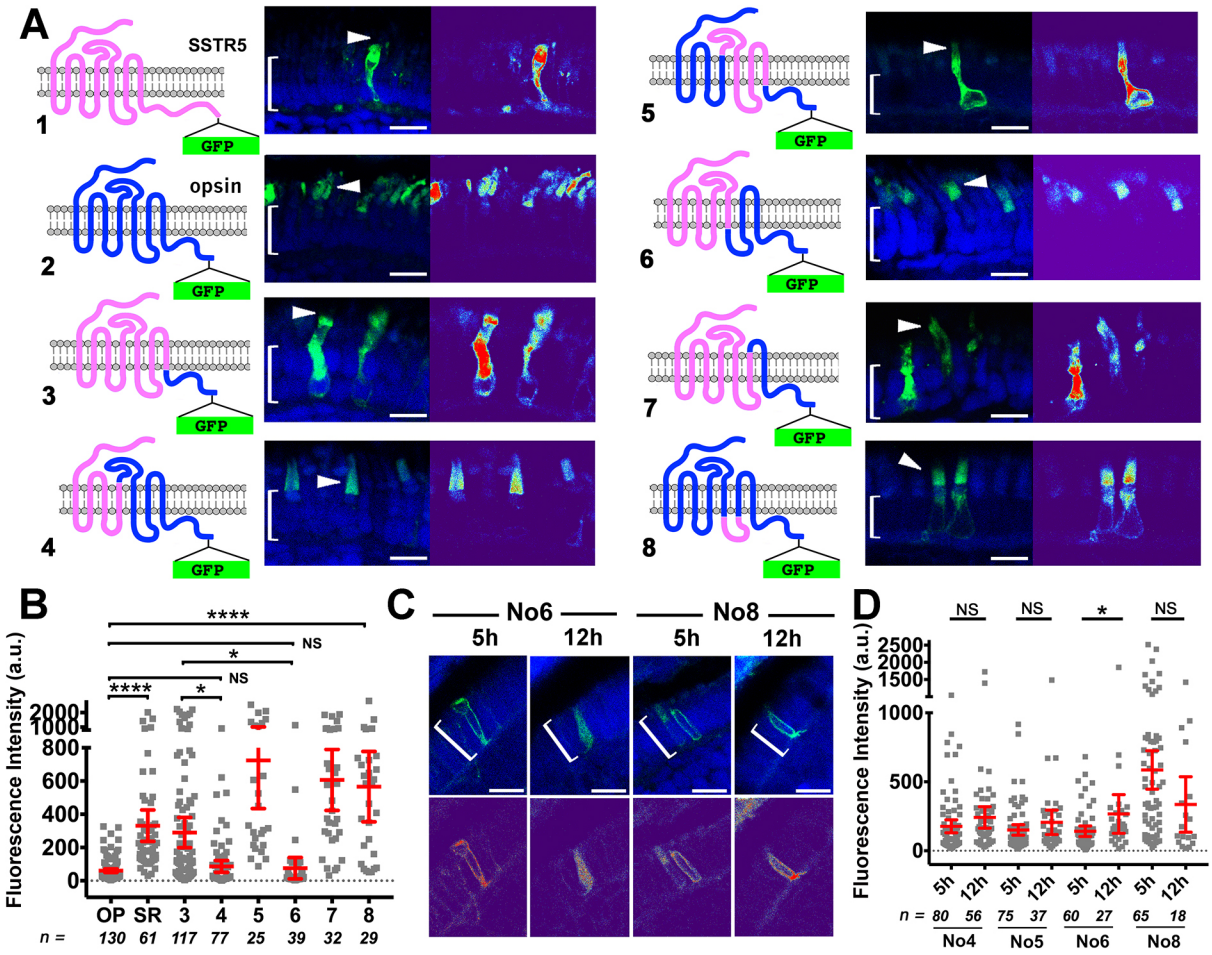

Fig. 3. Transport efficiency of opsin/Sstr5 hybrid GPCRs into the photoreceptor ciliary compartment. (A) Images of cryosections through zebrafish retinae expressing wild-type or hybrid GPCRs schematically represented to the left of each image. Brackets indicate the photoreceptor cell layer, and arrowheads point to OSs. In each panel, a confocal image (left) and a heat map (right) of GFP signal intensity are shown. (B) Quantification of the GFP signal intensity in photoreceptor cell bodies for wild-type and hybrid GPCRs shown in A. Data from four independent experiments are provided. (C) Images of cryosections showing the expression of two hybrid GPCRs in *oval*$^{-/-}$ mutant photoreceptors at 5 and 12 h post heat shock, as indicated in above panels. A confocal image (top) and a heat map (bottom) of GFP signal intensity are shown. (D) Quantification of GFP signal intensity in the cell bodies of *oval*$^{-/-}$ mutant photoreceptors expressing four hybrid GPCRs at 5 and 12 h post heat shock as indicated. Data are mean±95% c.i. from four independent experiments. In B and D each dot represents a single photoreceptor. Sample sizes are shown in italics below the horizontal axis. *<0.05; ****<0.0001; ns, not significant (ANOVA). a.u., arbitrary units. Scale bars: 10 µm.

Journal of Cell Science (2021) 134, jcs254995. doi:10.1242/jcs.254995

GFP signal could occur, however, by degradation of opsin/Sstr5-GFP hybrid polypeptides in the cell body. To test this, we expressed four hybrid constructs: two that are efficiently transported to the ciliary outer segment (Fig. 3A, constructs 4 and 6) and two that are not (Fig. 3A, constructs 5 and 8) in photoreceptors of *oval* (*ovl*) mutants. We showed previously that the *ovl*^{tz288b} strain harbors a mutation in the *ift88* gene that causes complete loss of the photoreceptor OS (Tsujikawa and Malicki, 2004). In the absence of the OS, opsin/Sstr5-GFP hybrids remain trapped in the cell body (Fig. 3C). We compared cytoplasmic expression levels of opsin/Sstr5-GFP hybrid constructs at 5 and 12 h post heat shock. We did not see statistically significant loss of GFP signal for any of the fusion constructs tested (Fig. 3D). Some signal loss between 5 and 12 h, albeit not statistically significant, was seen for hybrid 8. For hybrid 6, a small but statistically significant increase of signal was observed. These findings indicate that degradation is not a factor that significantly contributes to the rate of signal loss from the photoreceptor cell body in our assay. Moreover, we did not observe a relationship between the overall expression level and the rate of GFP signal loss from the cell body: although hybrid 8 was expressed at a higher level compared to the others, hybrid 5 was not, and yet it was inefficiently transported to the OS (Fig. 3D). Finally, we did not see a statistically significant photoreceptor cell loss for any construct between 5 and 12 h post heat shock (Fig. S3E). Cell loss is thus unlikely to account for differences in cell body GFP signal level. Taken together, these findings reveal that opsin transport into the OS requires a targeting sequence in the IC3 of rod opsin.

To define sequences sufficient to mediate OS targeting, we inserted rod opsin IC3 and CT44 into Sstr5 (construct 9; Fig. 4). This hybrid GPCR failed to localize to the OS, indicating that these two fragments of opsin sequence are not sufficient to target opsin to the OS. Similarly, a hybrid that, in addition to IC3 and CT44, contains helix 6 from opsin (Fig. 4A,C; construct 11) was not efficiently targeted to the OS, and substitution of opsin helix 6 in hybrid 6 with the Sstr5 sequence (Fig. 4A; hybrid 13) also impaired targeting to the ciliary compartment (Fig. 4C). These results suggest that the rod opsin transport mechanism involves both helices 6 and 7. Coherently, based on the opsin crystal structure (Park et al., 2008; Palczewski et al., 2000), these helices are close to each other and may interact to maintain opsin conformation and the relative positions of IC3 and CT44. To narrow down which parts of helices 6 and 7 are required for the ciliary targeting of opsin, we constructed a hybrid containing the N-terminal half of helix 6 and the C-terminal half of helix 7 from rod opsin in addition to opsin IC3 and CT44 (Fig. 4A, construct 14). We found that this configuration of opsin sequences was sufficient to mediate OS targeting with the same efficiency as the full-length sequence (Fig. 4C).

Studies of SSTR3 identified a conserved motif in IC3 necessary for ciliary targeting (Berbari et al., 2008). To test whether it is also required for opsin targeting, we deleted this motif (AAAQQQ) from the full-length rod opsin (construct 12, Fig. 4B). In contrast to SSTR3, this deletion did not affect OS targeting in photoreceptors (Fig. 4D). Thus, we were interested in which particular motif within IC3 is essential for its role with regard to OS targeting, as the common ciliary targeting motif appeared to be redundant for

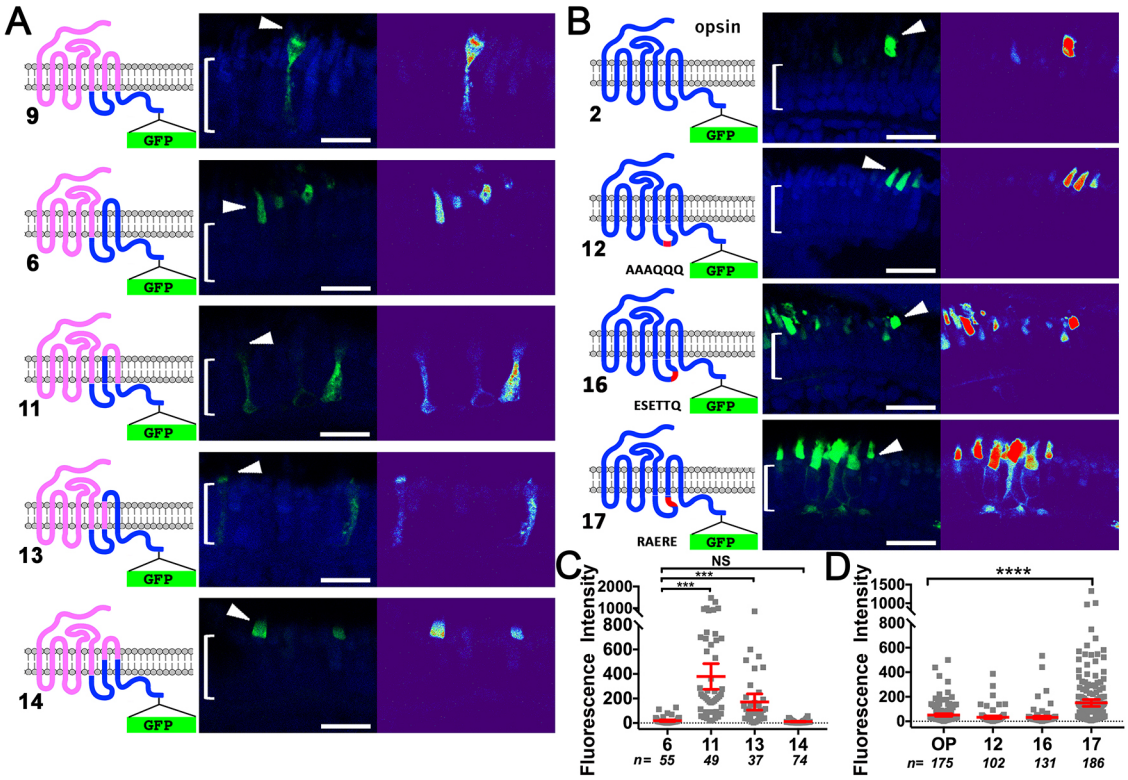

Fig. 4. Transport efficiency of opsin/Sstr5 hybrid GPCRs. (A,B) Images of cryosections through zebrafish retinae expressing wild-type or hybrid GPCRs schematically represented to the left of each image. Brackets indicate the photoreceptor cell layer, and arrowheads point to OSs. In each panel, a confocal image (left) and a heat map (right) of GFP signal intensity are shown. (C) Quantification of the GFP signal intensity in photoreceptor cell bodies for hybrid GPCRs shown in A. (D) Quantification of the GFP signal intensity in photoreceptor cell bodies for hybrid GPCRs shown in B. In C and D, data are mean±95% c.i. from three independent experiments, and each dot represents a single photoreceptor. Sample sizes are in italics below the horizontal axis. ***<0.001; ****<0.0001; ns, not significant (ANOVA). Scale bars: 10 µm.

Journal of Cell Science (2021) 134, jcs254995. doi:10.1242/jcs.254995

transport. To address this question, two additional deletion constructs (Fig. 4B,D; constructs 16 and 17) were tested, and the OS targeting defect was only observed in the absence of RAERE sequence, which is adjacent to helix 6, but the ESETTQ motif had no effect on opsin transport. It is possible that the defect in OS targeting observed in the RAERE mutant could simply be explained by a defect in protein folding and transport. To address this, we expressed these opsin variants in PAC2 cells and visualized their localization. All of the above opsin variants were able to escape from the endoplasmic reticulum (ER) and reach the plasma membrane as the full-length opsin (Fig. S4), suggesting that their mislocalization was not due to protein misfolding and ER retention. Taken together, these results define CT44, IC3 and parts of helices 6 and 7 as both necessary and sufficient to target rod opsin to the ciliary OS in vertebrate photoreceptors.

DISCUSSION

Cilia-targeting sequences have been identified for several proteins, including polycystins, cyclic nucleotide-gated channels, INPP5E and several GPCRs, including opsin (reviewed by Malicki and Avidor-Reiss, 2014). However, there does not appear to be a common ciliary targeting motif. GPCRs are to be thought to be transported to cilia by multiple mechanisms: although the C-terminal cytoplasmic tail appeared sufficient for opsin targeting to the OS, entirely different targeting motifs in the third cytoplasmic loop were shown to target other GPCRs to the ciliary compartment (Loktev and Jackson, 2013; Mukhopadhyay et al., 2013; Berbari et al., 2008). Targeting motifs found in other GPCRs appeared irrelevant to opsin because the opsin cytoplasmic tail seemed sufficient to target *Xenopus* opsin to the ciliary compartment (Tam et al., 2000). Conversely, opsin C-terminal targeting motifs, such as VxPx, are poorly conserved in SSTRs, if at all, supporting the idea that opsins use different targeting mechanisms compared to other GPCRs. In addition, the VxPx motif was shown to have negative effects on primary cilia targeting (Geneva et al., 2017), suggesting distinct transport mechanisms act in different cell types. However, our data establish that in our model system the third intracellular loop of opsin is essential for the targeting towards photoreceptor ciliary compartments, implying that at least some aspects of opsin transport are closely related to those of other GPCRs.

The AX[S/A]XQ motif, previously identified in other GPCRs and conserved in the opsin sequence, was not, however, necessary for opsin transport in our assay. This is not entirely unexpected as ciliary targeting motifs in the IC3 of GPCRs vary substantially: the [R/K][I/L]W motif of NPY2R and [I/V]KARK of GPR161 are not related to the ciliary targeting sequence of SSTR3, and do not display clear similarity to each other apart from the presence of basic and hydrophobic residues (Mukhopadhyay et al., 2013; Loktev and Jackson, 2013). In addition, in agreement with our analysis, mutating the SSTR3-related motif does not affect the ciliary trafficking of GPR83 (Loktev and Jackson, 2013). Rod opsin is thus likely to have yet another set of targeting motifs in IC3. Indeed, our data suggests that the RAERE motif in the IC3 is necessary for opsin OS targeting. Work by several groups has shed light on the proteins that facilitate opsin transport, including Arf4 (Deretic et al., 2005; Mazelova et al., 2009), ASAP1, Rab8 and Rab11 (Wang et al., 2012) and IFTs (Keady et al., 2011; Crouse et al., 2014). It has been shown that Arf4 binds to the VxPx motif and ASAP1 binds to the FR motif at the opsin C termini (Fig. 5E). However, some of these components appear to be dispensable *in vivo* for opsin transport (Pearring et al., 2017; Ying et al., 2016). Our data suggest the IC3 potentially could be a new binding site for trafficking machinery. The IC3 was suggested as a binding site for TULP3 and RABL2, which have been shown to act as adaptors (Barbeito et al., 2020; Badgandi et al., 2017) for the transport of several GPCRs to the primary cilium. In the future, the role of IC3 as an interacting site for opsin transport will need to be further addressed by biochemical approaches.

Our studies show that in addition to targeting motifs in the third intracellular loop, parts of helices 6 and 7 on the intracellular side of the membrane also contribute to opsin transport (summarized in Fig. 5). In crystal structures (Palczewski et al., 2000; Park et al., 2008), these helices localize close to each other (Fig. 5B-D) and their interactions may be necessary to position IC3 and/or helix 8 in a way that facilitates interactions with components of the ciliary transport machinery (Fig. 5E). Interestingly, both helix 6 and helix 7 contain residues (Met253, Met257, Ile305 and others; Fig. 5D) that are well conserved among ciliary but not rhabdomeric opsins (Arendt et al., 2004), supporting the conclusion that these helices are involved in OS targeting. Additionally, we show that segments of both helices are required to facilitate efficient OS targeting, consistent with the hypothesis that their interaction with each other is required.

A surprising conclusion of our analysis is that *Xenopus* C-terminal sequence functions as an OS targeting signal in zebrafish photoreceptors, whereas the homologous zebrafish sequence does not. The alignment of opsins from vertebrates (Fig. S1) shows that Met317 is conserved in all species examined, except *Xenopus*, in which it is substituted by leucine. This suggests that *Xenopus* opsin transport may be different from other vertebrates. Interestingly, we also observed that the human sequence and its leucine variant behave in the same way as the zebrafish constructs (Fig. S2B-D). At present, it is unclear why the leucine substitution could make such dramatic changes for OS targeting.

One possibility is that the *Xenopus* C-terminal tail has an unusually strong propensity to bind components of opsin transport machinery, whereas additional sequences are required for zebrafish and other opsins to achieve sufficient interactions. This would explain why *Xenopus* CT44 is efficiently targeted to the OS in zebrafish, but the homologous sequence from zebrafish does not behave in this way. *Xenopus* opsin transport may need to be significantly more efficient because the *Xenopus* rod OS is ∼30-fold larger than the mouse rod OS. In addition, the replenishment rate of the OS is higher in *Xenopus* (∼eightfold higher than in the mouse) compared to other species (Pearring et al., 2013).

An additional explanation for the ability of the *Xenopus* opsin C terminus to more efficiently target to the OS may be linked to the likelihood of opsin dimer formation. Several lines of evidence show that helix 8, together with helix 1, form one of the possible interfaces that mediate interactions between opsin molecules. First, an opsin homodimer crystal structure [Protein Data Bank (PBD) ID 3CAP] shows that helices 8 and 1 are positioned at the dimerization interface (Park et al., 2008). Second, chemical cross-linking in bovine rod OS membranes identified a Cys316-Cys316 crosslink between helix 8 of two monomers (Knepp et al., 2012), again suggesting that helix 8 mediates dimerization. Notably, Cys316 is adjacent to Leu317, which we identified as essential for efficient XCT44 targeting to the OS. Finally, delivery of helix 8 peptide to mouse photoreceptors mislocalizes opsin, most likely due to interference with dimerization (Zhang et al., 2016). The alignment of opsins from vertebrates (Fig. S1) shows that Met317 is conserved in all species examined, except *Xenopus*, in which it is substituted by leucine. This reveals that *Xenopus* opsin transport involves molecular features not shared with other vertebrates. In the light of evidence that helix 8 mediates opsin dimerization, an intriguing

Journal of Cell Science (2021) 134, jcs254995. doi:10.1242/jcs.254995

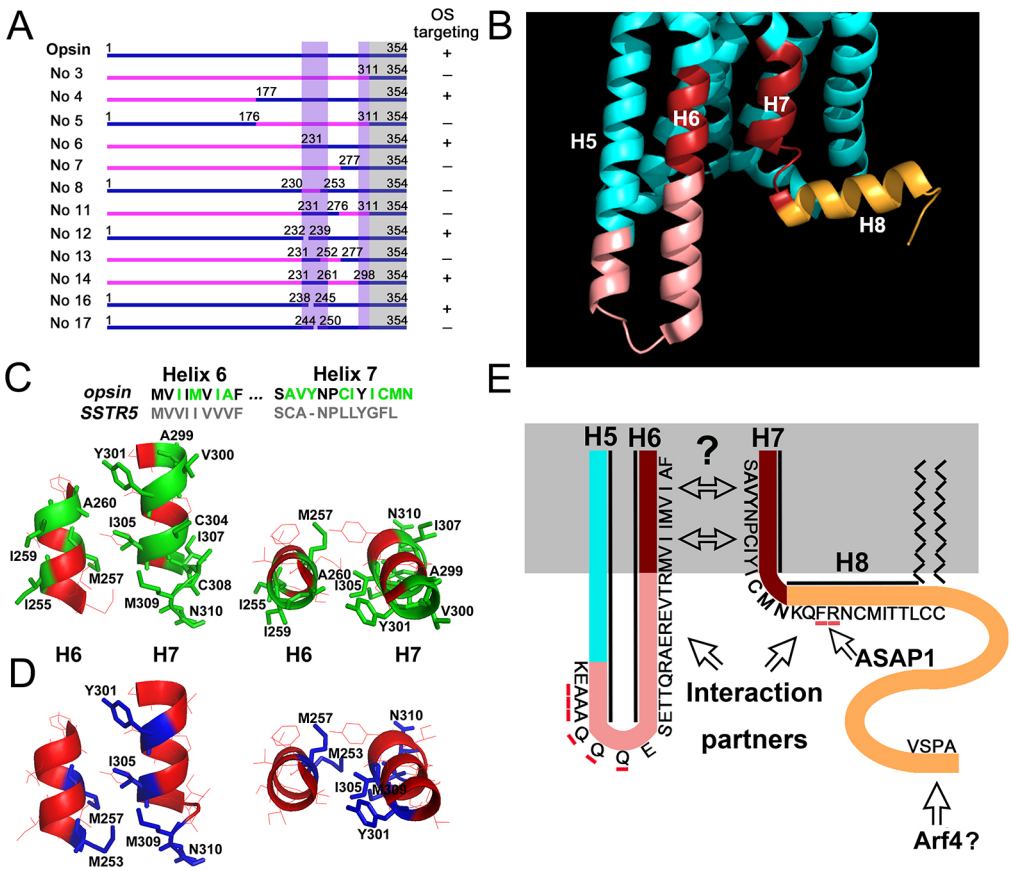

Fig. 5. Summary of opsin OS targeting motifs identified in this and previous studies. (A) Summary of results from Figs 3 and 4. Rod opsin sequences included in each construct are represented as blue horizontal bars, and Sstr5 sequences are depicted in pink. The first and last amino acid of each opsin fragment are numbered. Sequences necessary for the ciliary targeting of opsin are highlighted by vertical bars. The CT44 is indicated by a grey vertical bar. (B) The structure of opsin monomer based on X-ray crystallography (PDB: 3CAP). Fragments of transmembrane helices near the cytoplasmic face of the membrane and cytoplasmic loops are shown. Helix 8 is highlighted in orange, IC3 is in pink, and the portions of helices 6 and 7 that we found necessary for opsin transport are red. The remaining sequences are in cyan. (C,D) Regions of helices 6 and 7 necessary for opsin transport in side view and viewed along helix axis. (C) Amino acid side chains that differ between zebrafish rod opsin and zebrafish Sstr5 are numbered and depicted in green. (D) Amino acids that are conserved in ciliary but not in rhabdomeric opsins are numbered and depicted in blue. (E) Schematic representation of opsin features that are necessary and sufficient for the ciliary targeting of opsin. Sequences are color coded as in B. Helixes are indicated with solid black lines. The SSTR3 ciliary targeting motif and the FR motif are underlined in red. Arrows indicate potential interaction sites with proteins that facilitate opsin transport based on the work of several groups. In C and D, two amino acid substitutions were made: $V_{Bos}304$ to C_{Danio} and $V_{Bos}308$ to C_{Danio} to match the zebrafish sequence. In B-D, protein structure is visualized using PyMOL software.

possibility is that the *Xenopus* C-terminal tail has unusually strong propensity to dimerize and consequently is co-transported, or 'hitch-hikes', with the full-length wild-type protein. This would explain why *Xenopus* CT44 is efficiently targeted to the outer segment in zebrafish, but the homologous sequence from zebrafish does not behave in this way. A caveat is that multiple intradimeric contacts, including helices 1 and 2, 1 and 5, 1 and 8, 4 and 5, etc., have been identified by studies using electron microscopy and atomic force microscopy, as well as biochemical tools (Knepp et al., 2012; Jastrzebska et al., 2015; Liang et al., 2003; Ploier et al., 2016; Salom et al., 2006). Thus, whether opsin transport is in the form of dimer/oligomer, and whether helix 8 participates in, or is sufficient for, dimerization, are questions that remain to be addressed.

It is also possible that zebrafish opsin transport is different to that of higher vertebrates. For example, the zebrafish C-terminal sequence does not function well on its own or fused to the transmembrane domain of other GPCRs. However, the mouse rod opsin C-terminal sequence is able to direct part of peripherin, which lacks the C-terminal targeting signal, to the OS (Salinas et al., 2017; Tam et al., 2004; Salinas et al., 2013). At present, no study has directly tested how an isolated C-terminus behaves in mouse photoreceptors. However, it is worth noting that the RAERE motif is conserved in higher vertebrates as KAEKE and it is commonly shared within ciliary opsins but not within rhabdomeric opsins (Arendt et al., 2004). In the future, it will be important to directly test whether these residues are critical for opsin transport in higher vertebrates and whether they play a role in binding transport machinery.

MATERIALS AND METHODS

Zebrafish strains and maintenance

Zebrafish were maintained in the University of Sheffield aquarium facility in accordance with UK Home Office requirements. Embryos of AB, LWT (London wild-type) or Nacre lines were used for transient expression assays and transgenesis. The *ovl*^{tz288b} strain has been described previously (Tsujikawa and Malicki, 2004).

DNA constructs

Two transgenes were used to obtain spatial and temporal control of expression in photoreceptor cells: the Cre expression transgene and a conditional EGFP-CT44 transgene. To obtain rod-specific Cre expression, we cloned the 1.3 kb BglII-BamHI fragment from the XopsEGFP-N1

Journal of Cell Science (2021) 134, jcs254995. doi:10.1242/jcs.254995

plasmid (Fadool, 2003), containing the *Xenopus* rod opsin promoter, into the p5E-MCS vector. The resulting entry clone, p5E-XOPS-1324, pME-Cre and p3E-PolyA, were assembled into a pDestTol2CG2 destination vector using a Gateway reaction as described previously (Kwan et al., 2007). To construct conditional EGFP-S-CT44 transgenes, we synthesized a DNA fragment encoding a C-terminal fragment of EGFP fused to a 2xTEV-S-tag-CT44-polyA sequence (Integrated DNA Technologies) and combined it by overlap extension PCR with a lox2272-EGFP sequence. The PCR amplification product was inserted into the Gateway entry vector p3E-MCS (Invitrogen). The resulting entry clone was combined with p5E-hsp70 (Kwan et al., 2007) and pME-lox2272-mCherry(stop) in the pDestTol2pA2 destination vector using the Gateway reaction. Three versions of the conditional EGFP-CT44 transgene were made, containing zebrafish CT44 (CT44), *Xenopus* CT44 (XCT44) or a random 44 amino acid control sequence (CTC). The transgenes were termed as follows: Tg(XOPS-1324: Cre); Tg(hsp70: lox2272-mCherry-lox2272-EGFP-2xTEV-S-tag-XCT44); Tg(hsp70: lox2272-mCherry-lox2272-EGFP-2xTEV-S-tag-ZCT44); and Tg(hsp70:lox2272-mCherry-lox2272-EGFP-2xTEV-S-tag-CTC).

To test zebrafish and *Xenopus* CT44 cilia targeting sequences in transient expression assays, we first inserted EGFP between HindIII and EcoRI sites in the pME-MCS Gateway vector from the zebrafish Tol2 transgenesis kit (Kwan et al., 2007). The zebrafish CT44 sequence was then inserted downstream of EGFP between EcoRI and BamHI sites. The heat shock promoter and the polyA site were added using p5E-hsp70 and p3E-polyA entry clones from the same kit. We used a Gateway reaction to assemble the entry clones into the pDestTol2-CG2 destination vector, which includes *cmlc2:eGFP* as a transgenesis marker. Zebrafish/*Xenopus* hybrid CT44 sequences were assembled by PCR using forward primers encoding *Xenopus* or Zebrafish helix 8 or their mutant variants (Fig. 2). Zebrafish or *Xenopus* CT44 sequence was used as a template. Human constructs, AAR and their variants were made following the above strategy. Human and AAR sequences were obtained through DNA synthesis.

For opsin/Sstr5 hybrid experiments, the opsin reference construct was prepared by inserting EGFP after T336 in the ASTTASK sequence in zebrafish rod opsin (Rho; UniProtKB, P35359). An additional serine was introduced in this process generating the following insertion: AST-(EGFP)-STASK. This resulted in a fusion similar to that previously used to test bovine opsin transport (Moritz et al., 2001). The sstr5 reference construct was generated by appending EGFP to the C-terminus of the zebrafish sstr5 sequence (UniProtKB, Q6NV10), which was amplified from zebrafish cDNA. The melanopsin reference construct was cloned using the same procedure as for Sstr5. The zebrafish melanopsin gene (*opn4a*; Gene ID: 571624) was amplified from a cDNA clone (Source Bioscience, IRCYp5023J172D). Opsin-EGFP, Sstr5-EGFP and melanopsin-EGFP constructs were inserted into EcoRI/BamHI (opsin), HindIII/BamHI (sstr5) or XhoI/NotI (melanopsin) sites of the pME-MCS vector. All opsin/sstr5 and opsin/melanopsin hybrid constructs were made by overlap extension PCR and inserted into either EcoRI/BamHI (5, 8, 12, 16 and 17), HindIII/BamHI (3, 4, 6, 7, 9, 11, 13 and 14) or XhoI/BamHI (ML-No3) sites of the same vector. To generate the final heat shock promoter expression constructs, three entry clones, p5E-hsp70, pME-opsin/sstr5 and p3E-polyA were combined as above. The structure of all final constructs was confirmed by sequencing. Full amino acid sequences of opsin/Sstr5 and opsin/melanopsin are listed in Table S1.

Embryo injections and transgenesis

To generate stable transgenic lines and to perform transient expression assays, constructs were microinjected with Tol2 transposase as described previously (Kwan et al., 2007). While performing transient expression assays, in each experiment all constructs analyzed were injected during a single session. To obtain stable transgenic lines, XOPS-1324-Cre transgenic fish were selected at 3 days post fertilization (dpf) on the basis of cmlc:GFP expression. To generate fish transgenic for conditional EGFP-S-CT44 constructs, G0 larvae were screened 3 to 4 days after injection by heat shocking and selecting for mCherry expression 8 h post heat shock, using a high power fluorescence dissecting microscope. The same procedure was used in the F1 generation and mCherry$^+$ fish were raised to adulthood. Single transgene insertions that segregated in a Mendelian fashion were identified in subsequent generations.

Transient expression assays

In transient expression assays, 4-day-old wild-type larvae were heat shocked at 39°C for 30 min (CT44 analysis), 10 min (opsin/Sstr5 assays) or 20 min (opsin/melanopsin). Larvae with GFP$^+$ hearts were selected 5-6 h after heat shock and fixed 24 h post heat shock. Fixation, cryosectioning and imaging were performed as described previously (Malicki et al., 2016). Before imaging, sections were counterstained for 10 min in DAPI solution. For analysis in the *ovl*$^{-/-}$ mutant background, opsin/sstr5 hybrid constructs were injected into embryos originating from an *ovl*$^{+/-}$ heterozygote cross. Homozygous mutants were heat shocked at 3 dpf for 10 min and fixed 5 or 12 h post heat shock.

Assays using stable transgenic lines

For the analysis of opsin transport in wild-type retinae, single or double transgenics were heat shocked at 4 dpf for 30 min (EGFP-ZCT44) or 5 min (EGFP-XCT44), and analyzed at 5 h and 24 h post heat shock. Different heat shock times were used to compensate for the difference in the expression level of ZCT44 and XCT44 transgenes due to positional effects of transgene insertion. mCherry$^+$ larvae with green hearts were selected and processed for cryosectioning as above.

Image analysis

Single optical sections in the plane of retinal cryosections were acquired on an Olympus FV1000 confocal microscope and saved as oif format files, which were then processed using Fiji software. Signal intensity from the GFP channel was color-coded using a thermal lookup table. To measure signal intensity in photoreceptor cell bodies, a ∼2.5 µm wide line was drawn from the synapse to the OS base for each GFP$^+$ photoreceptor using Fiji software. Mean signal intensity in the area covered by the line was quantified and the resulting images were flattened and stored as TIFF files. To avoid signal overlap from neighboring cells, isolated GFP$^+$ cells were preferred for this analysis.

Statistical analysis

To analyze cytoplasmic GFP intensity in stable transgenic lines (Fig. 1), we log transformed signal intensity data and analyzed them using two-way ANOVA. Similarly, all other GFP intensity data were log transformed. The resulting data sets approximated normal distribution and were analyzed using ANOVA of mixed effects models assuming fish as a random effect. A Mann–Whitney test was used for data sets containing signal intensity, which was averaged per animal. *P*-values are indicated as follows: *<0.05; **<0.01; ***<0.001; and ****<0.0001.

Cell culture and immunofluorescence

PAC2 cells (Martin Lowe, University of Manchester, UK) were cultured at 28°C with 0.1% CO_2 and L-15 medium containing 10% fetal bovine serum and 1% Penicillin/Streptomycin. Transfections were performed according to the manufacturer's protocol for FuGENE HD transfection reagent (Promega, E2311). Heat shock was applied 4 h post transfection at 39°C, and cells were fixed with 4% paraformaldehyde/PBS 48 h after heat shock followed by 0.1% Triton X-100/PBS permeabilization. Permeabilization was not applied if followed by 4D2 staining. Bovine serum albumin/PBS (1%) was used for blocking and cells were stained by the following antibodies: anti-GRP78/Bip (Eames et al., 2013; 1:200, Abcam), anti-Rhodopsin Rho-4D2 (Salinas et al., 2017; 1:100, Abcam) and Alexa Fluor 568 anti-mouse IgG- or anti-rabbit IgG-conjugated secondary antibody (1:500, Invitrogen). Anti-GRP78/Bip antibody was applied to label the ER. Anti-Rho-4D2 antibody recognizes the N terminus of rod opsin. Without permeabilization, anti-Rho-4D2 only detects opsin molecules that reach the plasma membrane.

Acknowledgements

We thank Vadim Arshavsky, Elizabeth Smythe, Michael Cheetham, Ryan MacDonald, Stone Elworthy, Anton Nikolaev, Seth Blackshaw, Eleanor Markham and Daniel Williams for helpful comments on earlier versions of this work. Amy Spencer from the Statistical Services Unit helped with data analysis. We are grateful to Martin Lowe for providing the PAC2 cell line. We would like to dedicate this paper to the memory of Dr Jarema Malicki, who sadly and unexpectedly passed away in early 2019. This work was initiated and conducted under his inspired guidance.

Competing interests
The authors declare no competing or financial interests.

Author contributions
Methodology: J.J.M., X.F.; Validation: X.F., A.A.P., F.J.M.v.E, J.J.M.; Formal analysis: X.F., J.J.M.; Data curation: X.F.; Writing - original draft: X.F., J.J.M.; Writing - review & editing: X.F., A.A.P., F.J.M.v.E., J.J.M.; Supervision: A.A.P., F.J.M.v.E, J.J.M.; Project administration: J.J.M.; Funding acquisition: J.J.M.

Funding
This work was supported by Fight for Sight UK (1856/1857 to J.J.M.), the Medical Research Council (MR/N000714/1 to J.J.M.) and the Biotechnology and Biological Sciences Research Council (BB/R005192/1 to J.J.M.).

Supplementary information
Supplementary information available online at
https://jcs.biologists.org/lookup/doi/10.1242/jcs.254995.supplemental

Peer review history
The peer review history is available online at
https://jcs.biologists.org/lookup/doi/10.1242/jcs.254995.reviewer-comments.pdf

References

Arendt, D., Tessmar-Raible, K., Snyman, H., Dorresteijn, A. W. and Wittbrodt, J. (2004). Ciliary photoreceptors with a vertebrate-type opsin in an invertebrate brain. *Science* **306**, 869-871. doi:10.1126/science.1099955

Athanasiou, D., Aguila, M., Bellingham, J., Li, W., Mcculley, C., Reeves, P. J. and Cheetham, M. E. (2018). The molecular and cellular basis of rhodopsin retinitis pigmentosa reveals potential strategies for therapy. *Prog. Retin. Eye Res.* **62**, 1-23. 10.1016/j.preteyeres.2017.10.002

Badgandi, H. B., Hwang, S.-H., Shimada, I. S., Loriot, E. and Mukhopadhyay, S. (2017). Tubby family proteins are adapters for ciliary trafficking of integral membrane proteins. *J. Cell Biol.* **216**, 743-760. doi:10.1083/jcb.201607095

Barbeito, P., Tachibana, Y., Martin-Morales, R., Moreno, P., Mykytyn, K., Kobayashi, T. and Garcia-Gonzalo, F. R. (2020). HTR6 and SSTR3 ciliary targeting relies on both IC3 loops and C-terminal tails. *Life Sci. Alliance* **4**, e202000746. doi:10.26508/lsa.202000746

Berbari, N. F., Johnson, A. D., Lewis, J. S., Askwith, C. C. and Mykytyn, K. (2008). Identification of ciliary localization sequences within the third intracellular loop of G protein-coupled receptors. *Mol. Biol. Cell* **19**, 1540-1547. doi:10.1091/mbc.e07-09-0942

Berson, E. L., Rosner, B., Weigel-Difranco, C., Dryja, T. P. and Sandberg, M. A. (2002). Disease progression in patients with dominant retinitis pigmentosa and rhodopsin mutations. *Invest. Ophthalmol. Vis. Sci.* **43**, 3027-3036.

Besharse, J. C., Forestner, D. M. and Defoe, D. M. (1985). Membrane assembly in retinal photoreceptors. III. Distinct membrane domains of the connecting cilium of developing rods. *J. Neurosci.* **5**, 1035-1048. doi:10.1523/JNEUROSCI.05-04-01035.1985

Bessant, D. A. R., Khaliq, S., Hameed, A., Anwar, K., Payne, A. M., Mehdi, S. Q. and Bhattacharya, S. S. (1999). Severe autosomal dominant retinitis pigmentosa caused by a novel rhodopsin mutation (Ter349Glu). *Hum. Mutat.* **13**, 83. doi:10.1002/(SICI)1098-1004(1999)13:1<83::AID-HUMU12>3.0.CO;2-5

Chuang, J.-Z., Zhao, Y. and Sung, C.-H. (2007). SARA-regulated vesicular targeting underlies formation of the light-sensing organelle in mammalian rods. *Cell* **130**, 535-547. doi:10.1016/j.cell.2007.06.030

Crouse, J. A., Lopes, V. S., Sanagustin, J. T., Keady, B. T., Williams, D. S. and Pazour, G. J. (2014). Distinct functions for IFT140 and IFT20 in opsin transport. *Cytoskeleton* **71**, 302-310. doi:10.1002/cm.21173

Davies, W. I. L., Zheng, L., Hughes, S., Tamai, T. K., Turton, M., Halford, S., Foster, R. G., Whitmore, D. and Hankins, M. W. (2011). Functional diversity of melanopsins and their global expression in the teleost retina. *Cell. Mol. Life Sci.* **68**, 4115-4132. doi:10.1007/s00018-011-0785-4

Deretic, D., Williams, A. H., Ransom, N., Morel, V., Hargrave, P. A. and Arendt, A. (2005). Rhodopsin C terminus, the site of mutations causing retinal disease, regulates trafficking by binding to ADP-ribosylation factor 4 (ARF4). *Proc. Natl. Acad. Sci. USA* **102**, 3301-3306. doi:10.1073/pnas.0500095102

Eames, S. C., Kinkel, M. D., Rajan, S., Prince, V. E. and Philipson, L. H. (2013). Transgenic zebrafish model of the C43G human insulin gene mutation. *J. Diab. Investig.* **4**, 157-167. doi:10.1111/jdi.12015

Fadool, J. M. (2003). Development of a rod photoreceptor mosaic revealed in transgenic zebrafish. *Dev. Biol.* **258**, 277-290. doi:10.1016/S0012-1606(03)00125-8

Geneva, I. I., Tan, H. Y. and Calvert, P. D. (2017). Untangling ciliary access and enrichment of two rhodopsin-like receptors using quantitative fluorescence microscopy reveals cell-specific sorting pathways. *Mol. Biol. Cell* **28**, 554-566. doi:10.1091/mbc.e16-07-0549

Jastrzebska, B., Chen, Y., Orban, T., Jin, H., Hofmann, L. and Palczewski, K. (2015). Disruption of rhodopsin dimerization with synthetic peptides targeting an interaction interface. *J. Biol. Chem.* **290**, 25728-25744. doi:10.1074/jbc.M115.662684

Keady, B. T., Le, Y. Z. and Pazour, G. J. (2011). IFT20 is required for opsin trafficking and photoreceptor outer segment development. *Mol. Biol. Cell* **22**, 921-930. doi:10.1091/mbc.e10-09-0792

Kennedy, B. and Malicki, J. (2009). What drives cell morphogenesis: a look inside the vertebrate photoreceptor. *Dev. Dyn.* **238**, 2115-2138. doi:10.1002/dvdy.22010

Knepp, A. M., Periole, X., Marrink, S.-J., Sakmar, T. P. and Huber, T. (2012). Rhodopsin forms a dimer with cytoplasmic helix 8 contacts in native membranes. *Biochemistry* **51**, 1819-1821. doi:10.1021/bi3001598

Kwan, K. M., Fujimoto, E., Grabher, C., Mangum, B. D., Hardy, M. E., Campbell, D. S., Parant, J. M., Yost, H. J., Kanki, J. P. and Chien, C.-B. (2007). The Tol2kit: a multisite gateway-based construction kit for *Tol2* transposon transgenesis constructs. *Dev. Dyn.* **236**, 3088-3099. doi:10.1002/dvdy.21343

Lavail, M. M. (1973). Kinetics of rod outer segment renewal in the developing mouse retina. *J. Cell Biol.* **58**, 650-661. doi:10.1083/jcb.58.3.650

Lem, J., Krasnoperova, N. V., Calvert, P. D., Kosaras, B., Cameron, D. A., Nicolo, M., Makino, C. L. and Sidman, R. L. (1999). Morphological, physiological, and biochemical changes in rhodopsin knockout mice. *Proc. Natl. Acad. Sci. USA* **96**, 736-741. doi:10.1073/pnas.96.2.736

Liang, Y., Fotiadis, D., Filipek, S., Saperstein, D. A., Palczewski, K. and Engel, A. (2003). Organization of the G protein-coupled receptors rhodopsin and opsin in native membranes. *J. Biol. Chem.* **278**, 21655-21662. doi:10.1074/jbc.M302536200

Loktev, A. V. and Jackson, P. K. (2013). Neuropeptide Y family receptors traffic via the Bardet-Biedl syndrome pathway to signal in neuronal primary cilia. *Cell Rep.* **5**, 1316-1329. doi:10.1016/j.celrep.2013.11.011

Malicki, J. and Avidor-Reiss, T. (2014). From the cytoplasm into the cilium: bon voyage. *Organogenesis* **10**, 138-157. doi:10.4161/org.29055

Malicki, J. and Besharse, J. C. (2012). Kinesin-2 family motors in the unusual photoreceptor cilium. *Vision Res.* **75**, 33-36. doi:10.1016/j.visres.2012.10.008

Malicki, J., Pooranachandran, N., Nikolaev, A., Fang, X. and Avanesov, A. (2016). Analysis of the retina in the zebrafish model. *Methods Cell Biol.* **134**, 257-334. doi:10.1016/bs.mcb.2016.04.017

Matos-Cruz, V., Blasic, J., Nickle, B., Robinson, P. R., Hattar, S. and Halpern, M. E. (2011). Unexpected diversity and photoperiod dependence of the zebrafish melanopsin system. *PloS ONE* **6**, e25111. doi:10.1371/journal.pone.0025111

Mazelova, J., Astuto-Gribble, L., Inoue, H., Tam, B. M., Schonteich, E., Prekeris, R., Moritz, O. L., Randazzo, P. A. and Deretic, D. (2009). Ciliary targeting motif VxPx directs assembly of a trafficking module through Arf4. *EMBO J.* **28**, 183-192. doi:10.1038/emboj.2008.267

Moritz, O. L., Tam, B. M., Papermaster, D. S. and Nakayama, T. (2001). A functional rhodopsin-green fluorescent protein fusion protein localizes correctly in transgenic *Xenopus laevis* retinal rods and is expressed in a time-dependent pattern. *J. Biol. Chem.* **276**, 28242-28251. doi:10.1074/jbc.M101476200

Mukhopadhyay, S., Wen, X., Ratti, N., Loktev, A., Rangell, L., Scales, S. J. and Jackson, P. K. (2013). The ciliary G-protein-coupled receptor Gpr161 negatively regulates the sonic hedgehog pathway via cAMP signaling. *Cell* **152**, 210-223. doi:10.1016/j.cell.2012.12.026

Nagata, A., Hamamoto, A., Horikawa, M., Yoshimura, K., Takeda, S. and Saito, Y. (2013). Characterization of ciliary targeting sequence of rat melanin-concentrating hormone receptor 1. *Gen. Comp. Endocrinol.* **188**, 159-165. doi:10.1016/j.ygcen.2013.02.020

Nilsson, S. E. G. (1964). Receptor cell outer segment development and ultrastructure of the disk membranes in the retina of the tadpole (*Rana Pipiens*). *J. Ultrastruct. Res.* **11**, 581-620. doi:10.1016/S0022-5320(64)80084-8

Palczewski, K., Kumasaka, T., Hori, T., Behnke, C. A., Motoshima, H., Fox, B. A., Le Trong, I., Teller, D. C., Okada, T., Stenkamp, R. E. et al. (2000). Crystal structure of rhodopsin: a G protein-coupled receptor. *Science* **289**, 739-745. doi:10.1126/science.289.5480.739

Park, J. H., Scheerer, P., Hofmann, K. P., Choe, H.-W. and Ernst, O. P. (2008). Crystal structure of the ligand-free G-protein-coupled receptor opsin. *Nature* **454**, 183. doi:10.1038/nature07063

Pearring, J. N., Salinas, R. Y., Baker, S. A. and Arshavsky, V. Y. (2013). Protein sorting, targeting and trafficking in photoreceptor cells. *Prog. Retin. Eye Res.* **36**, 24-51. doi:10.1016/j.preteyeres.2013.03.002

Pearring, J. N., San Agustin, J. T., Lobanova, E. S., Gabriel, C. J., Lieu, E. C., Monis, W. J., Stuck, M. W., Strittmatter, L., Jaber, S. M., Arshavsky, V. Y. et al. (2017). Loss of Arf4 causes severe degeneration of the exocrine pancreas but not cystic kidney disease or retinal degeneration. *PLoS Genet.* **13**, e1006740. doi:10.1371/journal.pgen.1006740

Ploier, B., Caro, L. N., Morizumi, T., Pandey, K., Pearring, J. N., Goren, M. A., Finnemann, S. C., Graumann, J., Arshavsky, V. Y., Dittman, J. S. et al. (2016). Dimerization deficiency of enigmatic retinitis pigmentosa-linked rhodopsin mutants. *Nat. Commun.* **7**, 12832. doi:10.1038/ncomms12832

Pugh, E. and Lamb, T. (2000). Phototransduction in Vertebrate Rods and Cones. In *Handbook of Biological Physics* (ed. D. G. Stavenga, W. J. DeGrip and E. N. Pugh Jr), pp. 183-255. Elsevier Science B. V.

Röhlich, P. (1975). The sensory cilium of retinal rods is analogous to the transitional zone of motile cilia. *Cell Tissue Res.* **161**, 421-430. doi:10.1007/BF00220009

Salinas, R. Y., Baker, S. A., Gospe, S. M., III and Arshavsky, V. Y. (2013). A single valine residue plays an essential role in peripherin/rds targeting to photoreceptor outer segments. *PLoS ONE* **8**, e54292. doi:10.1371/journal.pone.0054292

Salinas, R. Y., Pearring, J. N., Ding, J.-D., Spencer, W. J., Hao, Y. and Arshavsky, V. Y. (2017). Photoreceptor discs form through peripherin-dependent suppression of ciliary ectosome release. *J. Cell Biol.* **216**, 1489-1499. doi:10.1083/jcb.201608081

Salom, D., Lodowski, D. T., Stenkamp, R. E., Le Trong, I., Golczak, M., Jastrzebska, B., Harris, T., Ballesteros, J. A. and Palczewski, K. (2006). Crystal structure of a photoactivated deprotonated intermediate of rhodopsin. *Proc. Natl. Acad. Sci. USA* **103**, 16123-16128. doi:10.1073/pnas.0608022103

Standfuss, J., Edwards, P. C., D'antona, A., Fransen, M., Xie, G., Oprian, D. D. and Schertler, G. F. X. (2011). The structural basis of agonist-induced activation in constitutively active rhodopsin. *Nature* **471**, 656. doi:10.1038/nature09795

Sung, C. H., Davenport, C. M., Hennessey, J. C., Maumenee, I. H., Jacobson, S. G., Heckenlively, J. R., Nowakowski, R., Fishman, G., Gouras, P. and Nathans, J. (1991). Rhodopsin mutations in autosomal dominant retinitis pigmentosa. *Proc. Natl. Acad. Sci. USA* **88**, 6481-6485. doi:10.1073/pnas.88.15.6481

Sung, C. H., Makino, C., Baylor, D. and Nathans, J. (1994). A rhodopsin gene mutation responsible for autosomal dominant retinitis pigmentosa results in a protein that is defective in localization to the photoreceptor outer segment. *J. Neurosci.* **14**, 5818-5833. doi:10.1523/JNEUROSCI.14-10-05818.1994

Tai, A. W., Chuang, J.-Z., Bode, C., Wolfrum, U. and Sung, C.-H. (1999). Rhodopsin's carboxy-terminal cytoplasmic tail acts as a membrane receptor for cytoplasmic dynein by binding to the dynein light chain Tctex-1. *Cell* **97**, 877-887. doi:10.1016/S0092-8674(00)80800-4

Tam, B. M., Moritz, O. L., Hurd, L. B. and Papermaster, D. S. (2000). Identification of an outer segment targeting signal in the COOH terminus of rhodopsin using transgenic Xenopus laevis. *J. Cell Biol.* **151**, 1369-1380. doi:10.1083/jcb.151.7.1369

Tam, B. M., Moritz, O. L. and Papermaster, D. S. (2004). The C terminus of peripherin/rds participates in rod outer segment targeting and alignment of disk incisures. *Mol. Biol. Cell* **15**, 2027-2037. doi:10.1091/mbc.e03-09-0650

Tokuyasu, K. and Yamada, E. (1959). The fine structure of the retina studied with the electron microscope. IV. Morphogenesis of outer segments of retinal rods. *J. Biophys. Biochem. Cytol.* **6**, 225-230. doi:10.1083/jcb.6.2.225

Tsujikawa, M. and Malicki, J. (2004). Intraflagellar transport genes are essential for differentiation and survival of vertebrate sensory neurons. *Neuron* **42**, 703-716. doi:10.1016/S0896-6273(04)00268-5

Wang, J., Morita, Y., Mazelova, J. and Deretic, D. (2012). The Arf GAP ASAP1 provides a platform to regulate Arf4 -and Rab11-sRab8-mediated ciliary receptor targeting. *EMBO J.* **31**, 4057-4071. doi:10.1038/emboj.2012.253

Ying, G., Gerstner, C. D., Frederick, J. M., Boye, S. L., Hauswirth, W. W. and Baehr, W. (2016). Small GTPases Rab8a and Rab11a are dispensable for rhodopsin transport in mouse photoreceptors. *PLoS ONE* **11**, e0161236. doi:10.1371/journal.pone.0161236

Young, R. W. (1967). The renewal of photoreceptor cell outer segments. *J. Cell Biol.* **33**, 61-72. doi:10.1083/jcb.33.1.61

Young, R. W. and Droz, B. (1968). The renewal of protein in retinal rods and cones. *J. Cell Biol.* **39**, 169-184. doi:10.1083/jcb.39.1.169

Zhang, T., Cao, L.-H., Kumar, S., Enemchukwu, N. O., Zhang, N., Lambert, A., Zhao, X., Jones, A., Wang, S., Dennis, E. M. et al. (2016). Dimerization of visual pigments in vivo. *Proc. Natl. Acad. Sci. USA* **113**, 9093-9098. doi:10.1073/pnas.1609018113

Zhao, C. and Malicki, J. (2011). Nephrocystins and MKS proteins interact with IFT particle and facilitate transport of selected ciliary cargos. *EMBO J.* **30**, 2532-2544. doi:10.1038/emboj.2011.165